High quality factor trapezoidal subwavelength grating waveguide micro-ring resonator

Zheng Wang*[a, b, †], Xiaochuan Xu*[c,†], D.L. Fan[a,d], Yaguo Wang[a, d] and Ray T. Chen*[a,b,c]
[a]Materials Science and Engineering Program, Texas Materials Institute, The University of Texas at Austin, Austin, TX USA 78712;
[b]Dept. of Electrical and Computer Engineering, The University of Texas at Austin, 10100 Burnet Rd., MER 160, Austin, TX USA 78758;
[c]Omega Optics, Inc., 8500 Shoal Creek Blvd., Bldg. 4, Suite 200, Austin, TX USA 78757;
[d]Dept. of Mechanical Engineering, University of Texas at Austin, Austin, TX USA 78712;
[†]These authors equally contributed to this work.

ABSTRACT

In recent decades, silicon photonics has attracted intensive research interest in optical communications due to its advantageous compact dimensions and high-volume manufacturability. Particularly, micro-ring resonators on silicon-on-insulator (SOI) platform have been widely exploited as a basic building block for a vast range of applications such as switches, modulators, and sensors. A majority of these applications involve light-matter interaction, which can be substantially enhanced by the high quality factor micro-ring resonators. However, conventional strip waveguide based micro-ring resonators suffer from the intrinsic dilemma in achieving high light confinement and strong light-matter interaction simultaneously. Subwavelength grating (SWG) waveguides, comprised of periodically interleaved high and low refractive index materials with a pitch less than one wavelength, have been demonstrated as a promising alternative. For SWG waveguides built on SOI wafers, the ratio of silicon and cladding materials can be engineered microscopically to achieve desired macroscopic properties. The control of these properties could potentially lead to significant performance improvements compared with conventional micro-ring resonators based photonic devices, such as filters and sensors. However, SWG waveguide based micro-ring resonators (SWGMRs) that have been demonstrated so far can only provide a moderate quality factor (~5600) with a large radius (e.g. 15 μm), which greatly jeopardize the wide spread research efforts in this area. In this paper, we propose to use trapezoidal silicon pillars to reduce the bend loss of SWGMRs to improve the quality factor. For the first time, we experimentally demonstrate the smallest SWGMR (the micro-ring radius equals to 5 μm) with an applicable quality factor as high as 11,500. This approach also can be applied to SWGMRs with larger radii for higher quality factors. We also experimentally demonstrated a 10 μm radius SWGMR that can provide a quality factor up to 45,000. Compared to SWGMRs built with conventional rectangular silicon pillars, the quality factors is increased by 4.6 times from a 5 μm radius SWGMR and 3 times from a 10 μm SWGMR radius, respectively.

Keywords: Subwavelength structures, Subwavelength grating waveguide, Micro-ring resonator

1. INTRODUCTION

In recent decades, photonic devices on silicon-on-insulator (SOI) platform have attracted intensive research interest due to the advantageous compact dimensions and high-volume manufacturability [1-5]. Particularly, micro-ring resonators on the SOI platform have been considered as a basic building block for a vast range of applications [6]. Numerous devices based on micro-ring resonators such as filters [7-10], switches [11-15], modulators [16-19], and sensors [20-23] have been demonstrated. However, the conventional strip waveguide based micro-ring resonators suffer from the intrinsic dilemma in having both high light confinement and strong light-matter interaction with environment. Specifically, a high confinement of light that ensures the desired low loss propagation also suggests limited light-matter interaction, which jeopardizes its performance. Recently, subwavelength grating (SWG) waveguides, comprised of periodically interleaved high and low refractive index materials with a pitch less than one wavelength, have been demonstrated as a promising solution to the aforementioned dilemmatic difficulties [24-28]. For SWG waveguides built on SOI wafers, the ratio of

* wangzheng@utexas.edu; xiaochuan.xu@omegaoptics.com; chenrt@austin.utexas.edu

Optical Interconnects XVI, edited by Henning Schröder, Ray T. Chen, Proc. of SPIE Vol. 9753, 97530P

silicon and cladding materials can be engineered microscopically to achieve desired macroscopic properties. The control of these properties could potentially lead to significant performance improvement compared with conventional micro-ring resonators based photonic devices, such as filters [29] and sensors [30]. However, the reported SWG waveguide based micro-ring resonators (SWGMR) can only provide a moderate quality factor (~5600) with a large micro-ring radius of 15 μm [30], with which it is difficult to build practical compact silicon photonics devices. To achieve an HQ-SWGMR, it is essential to reduce the intrinsic bend loss of an unloaded SWGMR. In this paper, we applied our geometrical tuning art using trapezoidal silicon pillars instead of conventional rectangular silicon pillars [31] to reduce the bend loss of SWGMRs and successfully achieved desired HQ-SWGMRs by design.

2. DESIGN AND OPTIMIZATION

The 3D schematic of a conventional rectangular SWG waveguide is shown in Fig.1(a), where Λ is the period of the SWG structure. l, w, and h are the length, width, and height of silicon pillars, respectively. SU-8 (n=1.58) is selected as the top cladding material. The period Λ is 300 nm and a typical silicon pillar with a geometry of $l \times w \times h$ = 150 nm × 500 nm × 250 nm has been selected. Quasi-TE polarization is investigated in this paper while the results can also be applied to Quasi-TM polarization. The schematic of an SWGMR built with trapezoidal silicon pillars (T-SWGMR) is shown in Fig. 1(b), where r and g denote the radius of the SWGMR and the center-to-center distance between the SWG bus waveguide and the curved SWG waveguide, respectively. Compared to conventional SWGMR fully built with rectangular silicon pillars (R-SWGMR), the SWGMR of a T-SWGMR will be built with trapezoidal silicon pillars to reduce bend loss while the SWG bus waveguide is still built with rectangular silicon pillars with the aforementioned geometry.

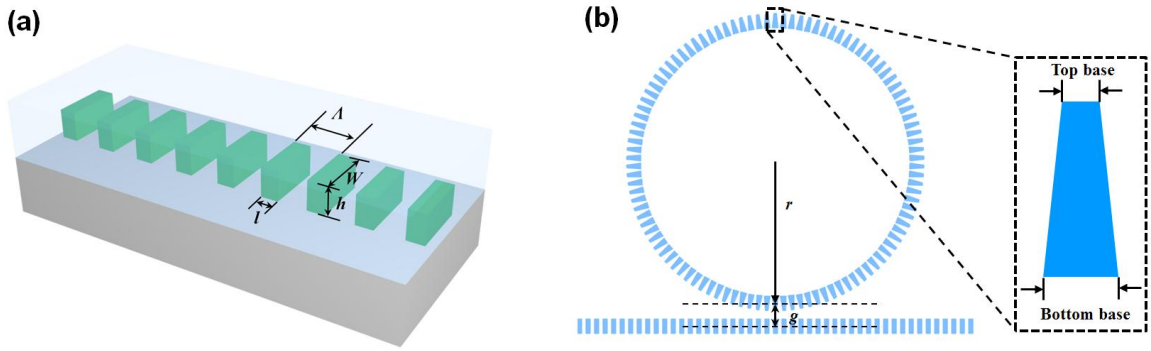

Fig. 1. (a) 3D schematic of a typical SWG waveguide (b) Schematic of a typical T-SWGMR

To achieve the T-SWGMR with the highest quality factor, the top and bottom base of trapezoidal silicon pillars need to be optimally tuned to minimize the bend loss. FullWAVE™ (developed by Synopsys Inc.), a 3D finite-difference time-domain method (FDTD) numerical simulator, has been adopted for optimization. The results are summarized in the contour plot shown in Fig. 2(a).

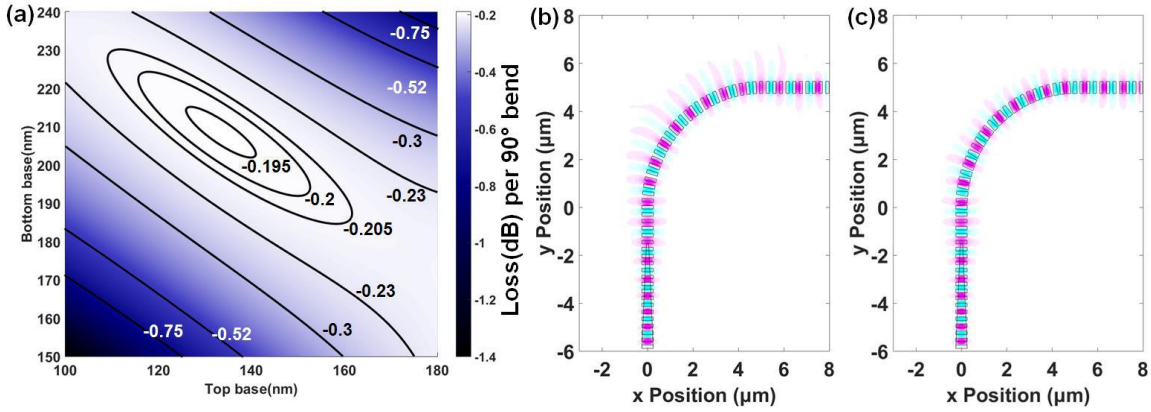

Fig. 2. (a) Contour plot of the bend loss of trapezoidal silicon pillars with different top bases and bottom bases. Top-view optical fields of SWG waveguide bends with (b) conventional rectangular silicon pillar and (c) optimally tuned trapezoidal silicon pillars.

It is found that a trapezoidal silicon pillar with 140 nm top base and 210 nm bottom base offers a minimum loss of 0.192 dB per 90 ° bend. It is 50.1% of the loss of an SWG waveguide bend built with conventional rectangular silicon pillars (0.383 dB per 90 ° bend). The top view of the optical fields (Re[Hz]) of 90° SWG waveguide bends with 5 μm radius are shown in Fig. 2(b) (conventional rectangular silicon pillars) and Fig. 2(c) (optimally tuned trapezoidal silicon pillars). One can readily find that the optical field of the SWG waveguide bend built with optimally tuned trapezoidal silicon pillars is better confined in the waveguide region (Fig. 2(b)) compared to the SWG waveguide bend built with conventional rectangular pillars (Fig. 2(c)). To validate that the coupling between SWGMR built with trapezoidal silicon pillars and SWG bus waveguide built with rectangular silicon pillars can be successfully triggered in a T-SWGMR, we simulated T-SWGMRs with various g values through 3D FDTD. Fig. 3(a) shows a typical simulated transmission spectrum of a T-SWGMR (r=5 μm and g=800 nm) and Fig. 3(b) shows a typical top view of the simulated optical field (Re[Hz]) of this T-SWGMR on resonance (r=5 μm and g=800 nm). One can find the FSR increases when the wavelength increases with a slope of 67 pm/nm. The dispersion of group refractive index implies a dispersion of effective index of the bend modes in SWGMRs, which can be exploited to design sensors based on the dispersive critical coupling condition[32].

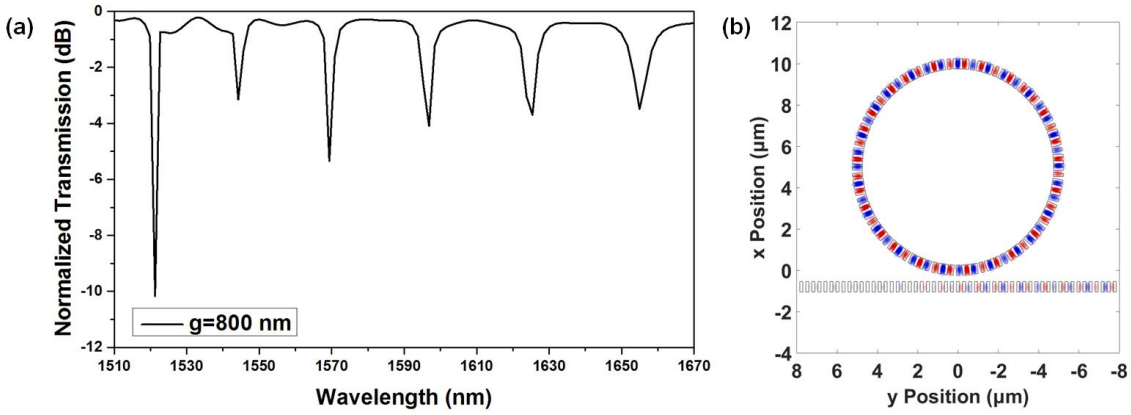

Fig. 3. (a) Typical simulated transmission spectrum of a T-SWGMR (r=5 μm and g=800 nm). (b) Typical top view of the simulated optical field (Re[Hz]) of a T-SWGMR (r=5 μm and g=800 nm).

3. EXPERIMENTAL DEMONSTRATION

We design our 5 μm radius T-SWGMRs based on the aforementioned optimally tuned trapezoidal silicon pillars with 140 nm top base and 210 nm bottom base. To compare with other groups' results, 10 μm radius T-SWGMRs are also designed. A control group of 5 μm radius and 10 μm radius R-SWGMRs are also prepared for internal comparison. The four types of SWGMRs (5 μm radius T-SWGMR, 5 μm radius R-SWGMR, 10 μm radius T-SWGMR and 10 μm radius R-SWGMR) have been fabricated for experimental demonstration. The devices are fabricated on an SOI wafer (SOITEC) consisting of a 250 nm thick top silicon layer and a 3 μm thick buried oxide layer. All structures are patterned in a single E-beam lithography (JEOL 6000 FSE) step at the nanofabrication facility center at the University of Texas at Austin. The patterns are then transferred into the silicon layer through reactive-ion-etching (PlasmaTherm 790). SU-8 2005(MicroChem Corp.) is spin-coated at 3000 rpm to form a 5 um thick top cladding. An overnight baking at 80 ℃ is applied to reflow the SU-8 for a tough infiltration [33]. Fig. 4(a) and 4(b) show typical SEM images of 5 μm radius R-SWGMR and T-SWGMR, respectively. Fig. 4(c) shows the typical high magnification SEM image of the coupling region between the bus waveguide and the micro-ring of a 5 μm radius T-SWGMR.

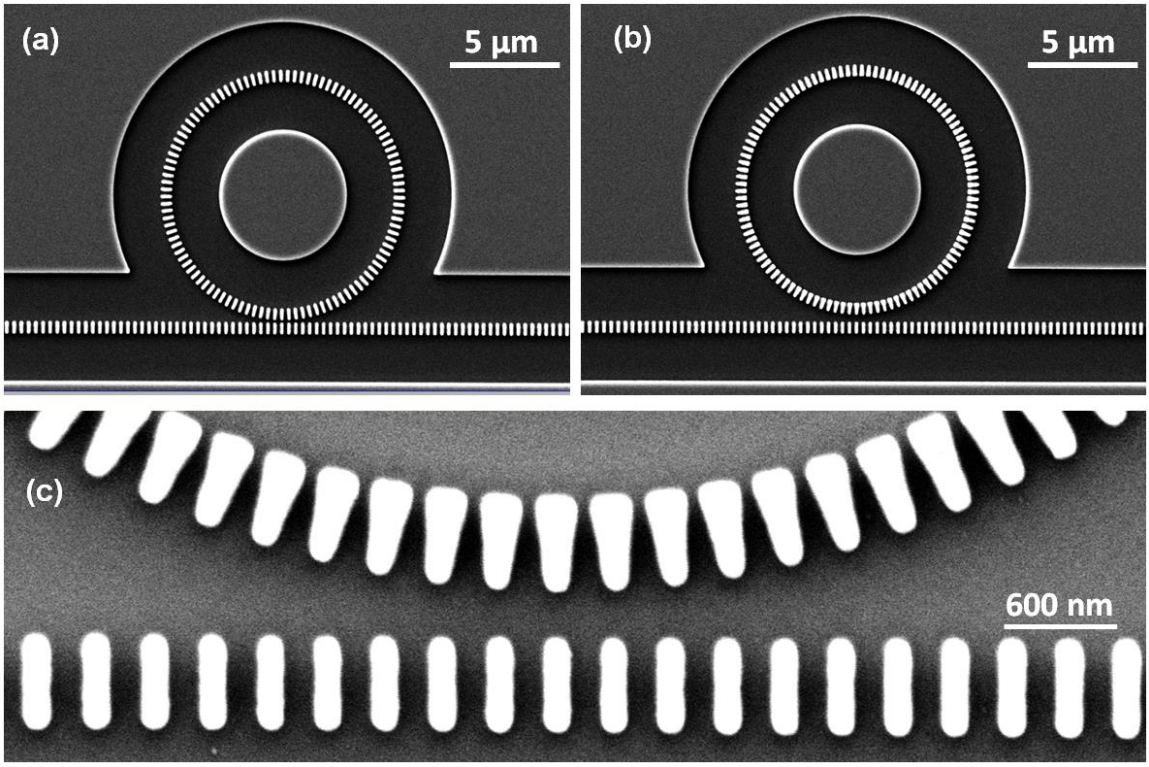

Fig. 4. (a) SEM image of 5 μm radius R-SWGMR. (b) SEM image of 5 μm radius T-SWGMR. (c) High magnification SEM image of the coupler of a 5 μm T-SWGMR.

After spin-coating the SU-8 cladding, the devices are tested in a customized grating coupler alignment system shown in Fig. 5(a). Two xyz stages are used to align the fibers to on-chip grating couplers and a camera mounted on another xyz stage is tilted at 45 °angle to visually assist in the alignment. Light from a broadband amplified spontaneous emission (ASE) source (1510 nm–1630 nm) is input to the device through a polarization maintaining fiber mounted on a tilting stage. After passing through the devices, light signal is collected by the output fiber, which is fed to an optical spectrum analyzer (OSA) to record the optical spectra. Fig. 5(b) and 5(c) show the transmission spectra of the four types of SWGMRs around the resonance of the highest quality factor. The 5 μm radius T-SWGMR can offer a resonance peak with a quality factor as high as 11,500, which 4.6 times to highest quality factor (~2,800) resonance peak that a 5 μm

radius R-SWGMR can offer. For 10 μm cases, a T-SWGMR can offer a resonance peak with a quality factor as high as 45,000, which 3 times to highest quality factor (~15,000) resonance peak that a 10 μm radius R-SWGMR can offer.

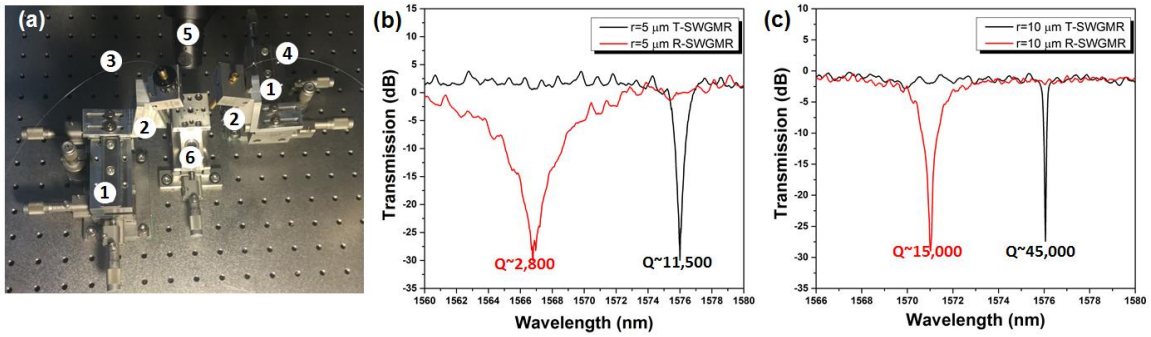

Fig. 5. (a)Grating coupler alignment system. (1)xyz stage. (2)Fiber mounts on tilting stage. (3)Input polarization maintaining fiber. (4)Output single mode fiber. (5) 45 ° tilted camera. (6)Adjustable sample stage. Transmission spectra of (b) 5 μm radius T-SWGMRs and R-SWGMRs, and (c) 10 μm radius T-SWGMRs and R-SWGMRs.

4. CONCLUSION

In conclusion, we successfully implemented our geometrical tuning art into HQ-SWGMRs. We demonstrated the smallest SWGMR (T-SWGMR architecture) with an applicable quality factor as high as 11,500. The quality factor can be increased to 45,000 for a 10 μm SWGMR(T-SWGMR architecture). Compared to the results reported earlier, where a quality factor of ~8,800 was obtained from 10 μm radius SWGMR (R-SWGMR architecture) [29], we successfully increase quality factor by five times. This study offers a promising platform for light-matter interaction research.

REFERENCES

[1] W. Bogaerts, R. Baets, P. Dumon *et al.*, "Nanophotonic waveguides in silicon-on-insulator fabricated with CMOS technology," J. Lightwave Technol., 23(1), 401-412 (2005).
[2] R. Soref, "The past, present, and future of silicon photonics," IEEE J. Sel. Topics Quantum Electron., 12(6), 1678-1687 (2006).
[3] M. Hochberg, N. C. Harris, R. Ding *et al.*, "Silicon photonics: the next fabless semiconductor industry," IEEE Solid State Circuits Mag., 5(1), 48-58 (2013).
[4] M. Lipson, "An exercise in self control," Nat. Photonics, 1(1), 18-19 (2007).
[5] T. Tsuchizawa, K. Yamada, H. Fukuda *et al.*, "Microphotonics devices based on silicon microfabrication technology," IEEE J. Sel. Topics Quantum Electron., 11(1), 232-240 (2005).
[6] W. Bogaerts, P. De Heyn, T. Van Vaerenbergh *et al.*, "Silicon microring resonators," Laser Photonics Rev., 6(1), 47-73 (2012).
[7] B. E. Little, S. T. Chu, H. A. Haus *et al.*, "Microring resonator channel dropping filters," J. Lightwave Technol., 15(6), 998-1005 (1997).
[8] Z. X. Qiang, W. D. Zhou, and R. A. Soref, "Optical add-drop filters based on photonic crystal ring resonators," Opt. Express, 15(4), 1823-1831 (2007).
[9] F. N. Xia, M. Rooks, L. Sekaric *et al.*, "Ultra-compact high order ring resonator filters using submicron silicon photonic wires for on-chip optical interconnects," Opt. Express, 15(19), 11934-11941 (2007).
[10] F. N. Xia, L. Sekaric, and Y. Vlasov, "Ultracompact optical buffers on a silicon chip," Nat. Photonics, 1(1), 65-71 (2007).
[11] V. R. Almeida, C. A. Barrios, R. R. Panepucci *et al.*, "All-optical control of light on a silicon chip," Nature, 431(7012), 1081-1084 (2004).

[12]V. R. Almeida, C. A. Barrios, R. R. Panepucci *et al.*, "All-optical switching on a silicon chip," Opt. Lett., 29(24), 2867-2869 (2004).
[13]P. Dong, S. F. Preble, and M. Lipson, "All-optical compact silicon comb switch," Opt. Express, 15(15), 9600-9605 (2007).
[14]S. Y. Cho, and R. Soref, "Interferometric microring-resonant 2x2 optical switches," Opt. Express, 16(17), 13304-13314 (2008).
[15]H. Wen, O. Kuzucu, T. G. Hou *et al.*, "All-optical switching of a single resonance in silicon ring resonators," Opt. Lett., 36(8), 1413-1415 (2011).
[16]Q. F. Xu, B. Schmidt, S. Pradhan *et al.*, "Micrometre-scale silicon electro-optic modulator," Nature, 435(7040), 325-327 (2005).
[17]B. G. Lee, B. A. Small, K. Bergman *et al.*, "Transmission of high-data-rate optical signals through a micrometer-scale silicon ring resonator," Opt. Lett., 31(18), 2701-2703 (2006).
[18]Q. F. Xu, B. Schmidt, J. Shakya *et al.*, "Cascaded silicon micro-ring modulators for WDM optical interconnection," Opt. Express, 14(20), 9430-9435 (2006).
[19]Q. F. Xu, S. Manipatruni, B. Schmidt *et al.*, "12.5 Gbit/s carrier-injection-based silicon micro-ring silicon modulators," Opt. Express, 15(2), 430-436 (2007).
[20]T. Claes, J. Girones Molera, K. De Vos *et al.*, "Label-Free Biosensing With a Slot-Waveguide-Based Ring Resonator in Silicon on Insulator," IEEE Photon. J., 1(3), 197-204 (2009).
[21]A. L. Washburn, L. C. Gunn, and R. C. Bailey, "Label-Free Quantitation of a Cancer Biomarker in Complex Media Using Silicon Photonic Microring Resonators," Anal. Chem., 81(22), 9499-9506 (2009).
[22]M. Iqbal, M. A. Gleeson, B. Spaugh *et al.*, "Label-Free Biosensor Arrays Based on Silicon Ring Resonators and High-Speed Optical Scanning Instrumentation," IEEE J. Sel. Topics Quantum Electron., 16(3), 654-661 (2010).
[23]Y. Z. Sun, and X. D. Fan, "Optical ring resonators for biochemical and chemical sensing," Anal. Bioanal. Chem., 399(1), 205-211 (2011).
[24]P. J. Bock, P. Cheben, J. H. Schmid *et al.*, "Subwavelength grating periodic structures in silicon-on-insulator: a new type of microphotonic waveguide," Opt. Express, 18(19), 20251-20262 (2010).
[25]V. Donzella, A. Sherwali, J. Flueekiger *et al.*, "Sub-wavelength grating components for integrated optics applications on SOI chips," Opt. Express, 22(17), 21037-21050 (2014).
[26]Y. L. Xiong, J. G. Wanguemert-Perez, D. X. Xu *et al.*, "Polarization splitter and rotator with subwavelength grating for enhanced fabrication tolerance," Opt. Lett., 39(24), 6931-6934 (2014).
[27]Y. Xiong, D.-X. Xu, J. Schmid *et al.*, "High extinction ratio and broadband silicon TE-pass polarizer using subwavelength grating index engineering," IEEE Photon. J., 7(5), 7802107 (2015).
[28]Y. Zhang, S. Han, S. Zhang *et al.*, "High Q and High Sensitivity Photonic Crystal Cavity Sensor," IEEE Photon. J., 7(5), 6802906 (2015).
[29]J. J. Wang, I. Glesk, and L. R. Chen, "Subwavelength grating filtering devices," Opt. Express, 22(13), 15335-15345 (2014).
[30]V. Donzella, A. Sherwali, J. Flueckiger *et al.*, "Design and fabrication of SOI micro-ring resonators based on sub-wavelength grating waveguides," Opt. Express, 23(4), 4791-4803 (2015).
[31]Z. Wang, X. C. Xu, D. L. Fan *et al.*, Geometrical tuning art for entirely subwavelength grating waveguide based integrated photonics circuits, submitted to Scientific Reports.
[32]W. Zhang, S. Serna, X. Le Roux *et al.*, "Highly sensitive refractive index sensing by fast detuning the critical coupling condition of slot waveguide ring resonators," Opt. Lett., 41(3), 532-535 (2016).
[33]H. Yan, Y. Zou, S. Chakravarty *et al.*, "Silicon on-chip bandpass filters for the multiplexing of high sensitivity photonic crystal microcavity biosensors," Applied Physics Letters, 106(12), (2015).